Hydrogen Storage Properties of Space-Confined $NaAlH_4$ Nanoparticles in Ordered Mesoporous Silica

Shiyou Zheng,[†] Fang Fang,[†] Guangyou Zhou,[†] Guorong Chen,[†] Liuzhang Ouyang,[‡] Min Zhu,[‡] and Dalin Sun*,[†]

Department of Materials Science, Fudan University, Shanghai 200433, China, and School of Materials Science and Technology, South China University of Technology, Guangzhou 510640, China

Received January 22, 2008. Revised Manuscript Received March 14, 2008

A method that is used by space-confining $NaAlH_4$ into the as-synthesized ordered mesoporous silica (OMS) is presented in the present work. $NaAlH_4$ in the pores of OMS is obtained by impregnation and drying techniques. It has been found that the space-confined $NaAlH_4$ in the pores of OMS shows the lower temperature and faster kinetics for dehydrogenation than that of the pristine $NaAlH_4$. Moreover, in the absence of a catalyst, the rehydrogenation in a dehydrogenated $NaAlH_4$ system with nanoscale particles and phases can be achieved even with the temperatures of 125−150 °C and the hydrogen pressures of 3.5−5.5 MPa. The physical limitation of the $NaAlH_4$ particles, as well as the resulting Al and NaH phases, to be nanoscale in size by the pores of OMS is believed to be responsible for these.

Introduction

Sodium alanate, $NaAlH_4$, has extensively been studied as a lightweight material for hydrogen storage,[1–4] following the discovery that the doping of transition metal catalysts in $NaAlH_4$ can significantly reduce its thermal stability.[5,6] The hydrogen storage in a doped $NaAlH_4$ system consists of two steps, involving the intermediate phases of Na_3AlH_6, NaH, and Al, as described by eqs 1 and 2.[7,8] In principle, the first step gives 3.7 wt % hydrogen and the second one 1.8 wt % upon heating.

$$NaAlH_4 \rightleftarrows \frac{1}{3}Na_3AlH_6 + \frac{2}{3}Al + H_2 \quad (1)$$

$$\frac{1}{3}Na_3AlH_6 \rightleftarrows NaH + Al + \frac{1}{2}H_2 \quad (2)$$

Although rehydrogenating the resulting NaH and Al phases in solid state back to the $NaAlH_4$ is possible, especially in the presence of Ti-containing catalysts,[9] the full reversibility of this rehydrogenation process is hardly achieved, which leads to a gradual deterioration in reversible hydrogen storage.[10–12] A reasonable explanation to this problem is that the interdiffusion between the NaH and the Al is hindered by either the segregation of small Al domains to large particles up to micrometer,[13,14] and/or the formation of some Al-related side products, such as Ti−Al, and Fe−Al alloys,[15–17] with the prolonged cycling under hydrogen. This explanation is supported by the formation of $NaAlH_4$, which would be remarkably enhanced once the cycled materials are regrounded into finer particles via ball milling.[18] Nevertheless, the problem is only mediated temporarily as the newly formed Al domains would inevitably aggregate again with the following cycling. It is therefore that further enhancement of the hydrogen storage properties of $NaAlH_4$ requires new methods. Recent studies show that an enhanced kinetics of hydrogen release is obtained by infusing ammonia borane (NH_3BH_3) in mesoporous silica,[19] and a reduced temperature for dehydrogenation by depositing $NaAlH_4$ nanoparticles on carbon nanofiber.[20]

In the present work, the idea of space-confined nanoparticles is proposed, which is obtained by confining $NaAlH_4$ into ordered mesoporous silica (OMS) in which the material is controlled to be nanoscale in size by the diameter and shape of the pores, and hence the phase segregation, such

* Corresponding author. Phone and fax: +86-21-65642873. E-mail: dlsun@fudan.edu.cn.
[†] Fudan University.
[‡] South China University of Technology.

(1) Schlapbach, L.; Züttel, A. *Nature* **2001**, *414*, 353.
(2) Grochala, W.; Edwards, P. P. *Chem. Rev.* **2004**, *104*, 1283.
(3) Orimo, S.; Nakamori, Y.; Eliseo, J. R.; Züttel, A.; Jensen, C. M. *Chem. Rev.* **2007**, *107*, 4111.
(4) Bogdanović, B.; Eberle, U.; Felderhoff, M.; Schüth, F. *Scr. Mater.* **2007**, *56*, 813.
(5) Bogdanović, B.; Schwickardi, M. *J. Alloys Compd.* **1997**, *253–254*, 1.
(6) Anton, D. L. *J. Alloys Compd.* **2003**, *356–357*, 400.
(7) Graetz, J.; Reilly, J. J.; Johnson, J. *Appl. Phys. Lett.* **2004**, *85*, 500.
(8) Chaudhuri, S.; Graetz, J.; Ignatov, A.; Reilly, J. J.; Muckerman, J. T. *J. Am. Chem. Soc.* **2006**, *128*, 11404.
(9) Wang, P.; Kang, X. D.; Cheng, H. M. *ChemPhysChem* **2005**, *6*, 2488.
(10) Bogdanović, P.; Brand, R. A.; Marjanovic, A.; Schwickardi, M.; Tolle, J. *J. Alloys Compd.* **2000**, *302*, 36.
(11) Sun, D.; Srinivasan, S. S.; Chen, G.; Jensen, C. M. *J. Alloys Compd.* **2004**, *373*, 265.
(12) Bogdanović, B.; Felderhoff, M.; Pommerin, A.; Schüth, F.; Spielkamp, N. *Adv. Mater.* **2006**, *18*, 1198.
(13) Singh, S.; Eijt, S. W. H.; Huot, J.; Kockelmann, W. A.; Wagemaker, M.; Mulder, F. M. *Acta Mater.* **2007**, *55*, 5549.
(14) Thomas, G. J.; Gross, K. J.; Yang, N. Y. C.; Jensen, C. M. *J. Alloys Compd.* **2002**, *330–332*, 702.
(15) Chaudhuri, S.; Muckerman, J. T. *J. Phys. Chem. B* **2005**, *109*, 6952.
(16) Fang, F.; Zhang, J.; Zhu, J.; Chen, G.; Sun, D.; He, B.; Zheng, W.; Wei, S. *J. Phys. Chem. C* **2007**, *111*, 3476.
(17) Fichtner, M.; Canton, P.; Kircher, O.; Léon, A. *J. Alloys Compd.* **2005**, *404–406*, 732.
(18) Sakintuna, B.; Lamari-Darkrim, F.; Hirscher, M. *Int. J. Hydrogen Energy* **2007**, *32*, 1121.
(19) Gutowska, A.; Li, L.; Shin, Y.; Wang, C. M.; Li, X. S.; Linehan, J. C.; Smith, R. S.; Kay, B. D.; Schmid, B.; Shaw, W.; Gutowski, M.; Autrey, T. *Angew. Chem., Int. Ed.* **2005**, *44*, 3578.
(20) Baldé, C. P.; Hereijgers, B. P. C.; Bitter, J. H.; de Jong, K. P. *Angew. Chem., Int. Ed.* **2006**, *45*, 3501.

10.1021/cm8002063 CCC: $40.75
Published on Web 05/21/2008

Scheme 1. Preparation Process for $NaAlH_4$ Nanoparticles Space-Confined in OMS

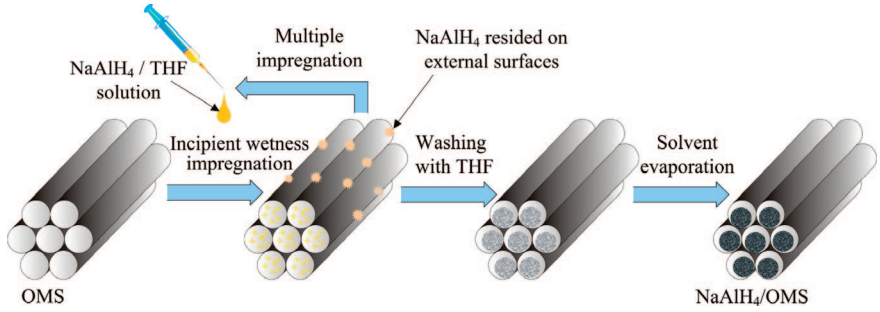

as Al and NaH, to be micrometer-sized particles during hydrogen release from $NaAlH_4$ may be prevented.

Experimental Section

Synthesis of OMS. OMS was synthesized according to the published procedure.[21–23] Pluronic ($EO_{20}PO_{70}EO_{20}$, P123, Aldrich) was dissolved in distilled water and HCl (37.5%), and the solution was stirred at 40 °C. Then tetraethoxysilane (TEOS, Aldrich 98%) was added into the mixture and stirred for 20 h and annealed at 100 °C for 24 h. The solid product was obtained by filtration, washed by water, air-dried at room temperature overnight, and calcined at 550 °C. As-synthesized, OMS was modified with methyl groups to avoid the reaction between $NaAlH_4$ and some silanol (Si−OH) groups.[24] The resulting OMS consists of mesopores with a diameter of around 10 nm, determined using the Barrett−Joyner−Halenda algorithm from the desorption branch of the nitrogen physisorption isotherm.

Preparation of $NaAlH_4$ Nanoparticles in OMS. $NaAlH_4$ in the pores of OMS was obtained by impregnation and drying techniques and is referred to here as $NaAlH_4$/OMS. The procedure is schematically shown in Scheme 1. First, $NaAlH_4$ (Sigma-Aldrich, 90%) was purified by using a procedure identical to that described previously.[25] One gram of purified $NaAlH_4$ was added to a beaker with 99 g of dried tetrahydrofuran (THF) with stirring at room temperature to produce a 1 wt % $NaAlH_4$ content solution ($NaAlH_4$/THF solution). The solution was added via wetness impregnation to 1 g of as-obtained OMS and subsequently heated up to 50 °C for 1 h. The treatment procedures were repeated five times with decreasing amounts of $NaAlH_4$/THF solution (first, 7 g; second, 6 g; third, 5 g; fourth, 4 g; fifth, 3 g). After that, 5 mL of dried THF was added to the flask to clean away the $NaAlH_4$ deposition on the external surface of OMS. This step was carried out no less than three times. The resulting sample was dried in a vacuum for 48 h, and around 20 wt % $NaAlH_4$ was determined to be loaded into the mesopores of OMS by measuring the change in mass before and after loading. All the handlings of the samples were carried out in a glovebox with an argon atmosphere.

Characterization. Scanning electron microscopy (SEM) images were obtained on an Hitachi S-4700, Japan, operating at 15 kV and equipped with an energy dispersive X-ray spectrometer (EDS). X-ray diffraction (XRD) patterns were recorded on a Rigaku D/max 2400, Japan, with Cu Kα radiation in the 2θ range from 5 to 80°. Identical to the procedure described elsewhere,[26] the samples for XRD studies were smeared on a glass slide in an argon glovebox and then covered with Scotch tape to prevent reaction with water and/or oxygen during measurement. High-resolution transmission electron microscopy (HRTEM) observation was carried out on a JEOL JEM-2100F, Japan, with an acceleration voltage of 200 kV, equipped with an EDS unit. The samples for HRTEM were prepared by dispersing in a dried THF solvent and then spreading on a holey carbon film supported on a copper grid. Differential scanning calorimetry (DSC) and thermogravimetry (TG) were performed simultaneously on a Netzsch STA 409 PC, Germany, with a heating rate of 5 °C/min and highly pure Ar as the purge gas. De-/rehydrogenation were carried out using an automated Sieverts' apparatus (AMC Gas Reaction Controller). The dehydrogenation was performed against a back pressure of 10 Pa. For the purpose of comparison, the masses of silica were excluded in the determination of the hydrogen amount released from the samples that contained OMS. The samples were exchanged into the SEM, XRD, HRTEM, and DSC-TG equipment by means of a device that maintained an Ar overpressure during the transfer process.

Results and Discussion

Structure Analysis. The surface morphologies of the as-obtained samples before and after washing with THF are compared in Figure 1a,b, showing that the surfaces of the OMS became cleaner and the $NaAlH_4$ particles that previously existed on the surfaces were washed away. Therefore, it is safe to deduce that, after washing, the remaining $NaAlH_4$ is mostly located inside the pores of the OMS, although the possibility of $NaAlH_4$ with very limited amounts on the OMS surface cannot be absolutely excluded. The EDS elemental maps for the $NaAlH_4$/OMS are also displayed in Figure 1c−f. The Si map follows the structure of the OMS, and the Na and Al ones coincide well with the Si map. This suggests that the $NaAlH_4$ particles are well-dispersed in the $NaAlH_4$/OMS.

To reveal the variation in phase component in the $NaAlH_4$/OMS before and after dehydrogenation by XRD, a physical mixture of OMS and $NaAlH_4$ (denoted as OMS doped-$NaAlH_4$ hereafter), corresponding to the gross composition of the $NaAlH_4$/OMS, was additionally prepared by mechanical grinding and used as the reference sample. XRD patterns for the samples of $NaAlH_4$/OMS, OMS, and OMS doped-$NaAlH_4$ are compared in Figure 2. Surprisingly, the peaks belonging to $NaAlH_4$ are not observed in the $NaAlH_4$/OMS

(21) Schüth, F. *Chem. Mater.* **2001**, *13*, 3184.
(22) Zhang, H.; Sun, J.; Ma, D.; Bao, X.; Klein-Hoffmann, A.; Weinberg, G.; Su, D.; Schlögl, R. *J. Am. Chem. Soc.* **2004**, *126*, 7440.
(23) Kochrick, E.; Krawiec, P.; Schnelle, W.; Geiger, D.; Schappacher, F. M.; Pöttgen, R.; Kaskel, S. *Adv. Mater.* **2007**, *19*, 3021.
(24) Hsueh, H.; Yang, C.; Zink, J. I.; Huang, M. H. *J. Phys. Chem. B* **2005**, *109*, 4404.
(25) Sun, D.; Srinivasan, S. S.; Kiyobayashi, T.; Kuriyama, N.; Jensen, C. M. *J. Phys. Chem. B* **2003**, *107*, 10176.
(26) Sun, D.; Kiyobayashi, T.; Takeshita, H. T.; Kuriyama, N.; Jensen, C. M. *J. Alloys Compd.* **2002**, *337*, L8.

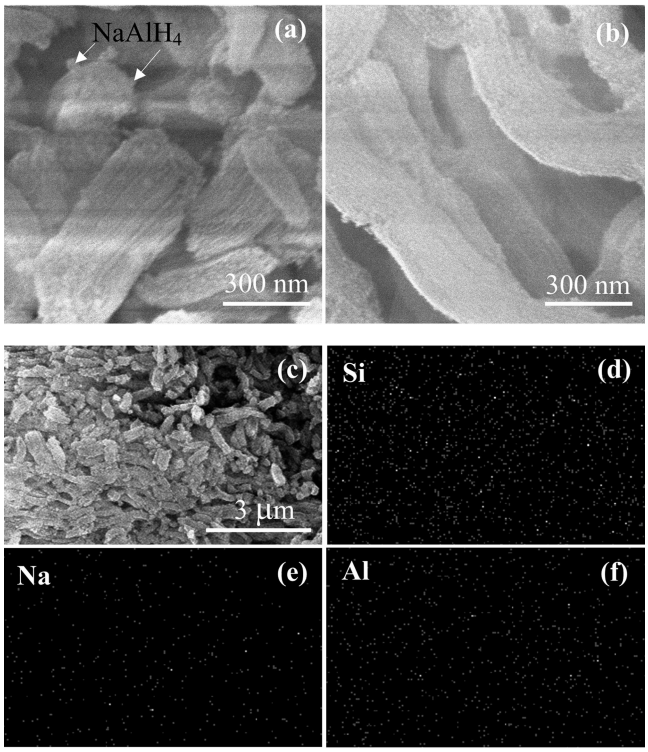

Figure 1. SEM images of the samples: (a) $NaAlH_4$/OMS before washing and (b) $NaAlH_4$/OMS after washing, and the corresponding EDS maps of Si, Na, and Al for image (c).

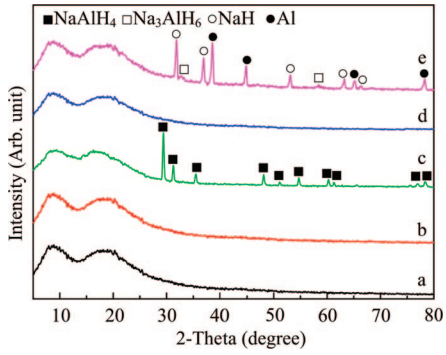

Figure 2. XRD patterns of the samples: (a) $NaAlH_4$/OMS, (b) OMS, (c) OMS doped-$NaAlH_4$, (d) $NaAlH_4$/OMS after dehydrogenation, and (e) OMS doped-$NaAlH_4$ after dehydrogenation.

(Figure 2a), whose pattern is almost identical to that of the OMS (Figure 2b), showing only two broad peaks within the range of 5−25° from the amorphous silica.[27] But in the case of OMS doped-$NaAlH_4$, the sharp and intense peaks from the $NaAlH_4$ are clearly visible in Figure 2c. This difference suggests that when confined by the pores of OMS, the $NaAlH_4$ in $NaAlH_4$/OMS is in an amorphous state and/or very fine crystallites. After dehydrogenation, no change in the pattern is observed for the $NaAlH_4$/OMS sample (Figure 2d), but the peaks of the NaH, Al, and Na_3AlH_6 phases are identified in the OMS doped-$NaAlH_4$ one (Figure 2e). This implies that, with the hydrogen release from the $NaAlH_4$, the resulting NaH and Al phases may also be in an amorphous state and/or very fine crystallites in the $NaAlH_4$/OMS sample.

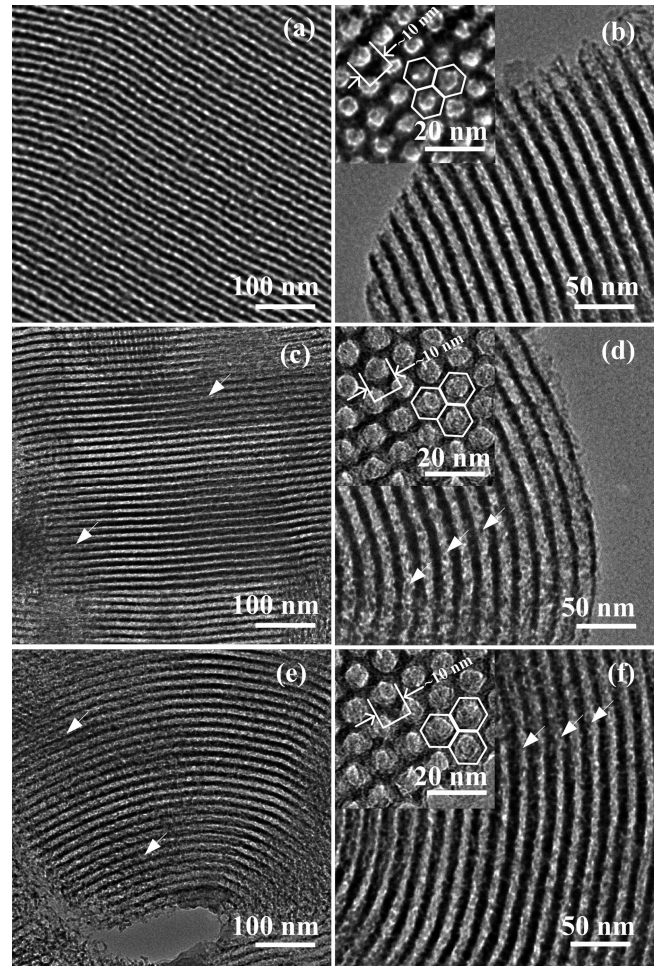

Figure 3. HRTEM micrographs of the OMS (a, b), the $NaAlH_4$/OMS (c, d), and the dehydrogenated $NaAlH_4$/OMS (e, f).

The microstructures of the OMS, and the $NaAlH_4$/OMS before and after dehydrogenation, were further characterized by HRTEM and presented in Figure 3, from which three features can be observed: (i) the initial OMS has well-defined mesoporous arrays about 10 nm in diameter, as shown in Figure 3a,b. This pore structure of the OMS matrix remains intact in the $NaAlH_4$/OMS (see Figure 3c,d), even undergoing a dehydrogenation process at 270 °C (see Figure 3e,f). These give the proof of thermal stability of the synthesized OMS sample in the following experiments. (ii) Comparing Figure 3a,b with Figure 3c,d, one can see that the $NaAlH_4$/OMS sample showed many dark domains and spots (marked by arrows) in Figure 3c,d inside the mesoporous arrays of the OMS. This indicates the $NaAlH_4$ particles were indeed loaded into the OMS. The images inserted in Figure 3b,d are the cross-section views along the [0 0 1] zone axis of OMS, showing the hexagonal mesoporous structure typical for OMS.[28] Moreover, the ends of the pores in the $NaAlH_4$/OMS are swollen, and darker in contrast than those in the OMS, providing more evidence that the mesopores of OMS were filled with $NaAlH_4$ in $NaAlH_4$/OMS. (iii) No significant difference is observed for the $NaAlH_4$/OMS sample before and after dehydrogenation at 270 °C (see Figure 3c−f. This suggests further that the resulting NaH and Al particles were

(27) Huo, Q.; Margolese, D. I.; Stucky, G. D. *Chem. Mater.* **1996**, *8*, 1147.

(28) Yuan, Z.; Zhou, W. *Chem. Phys. Lett.* **2001**, *333*, 427.

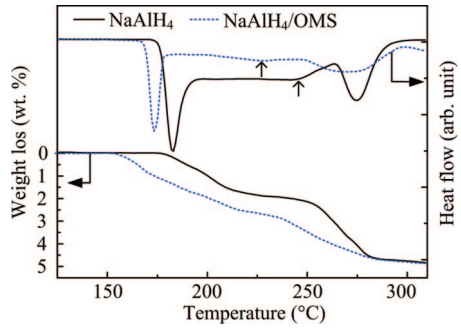

Figure 4. DSC and TG curves for the pristine $NaAlH_4$ and the $NaAlH_4$/OMS.

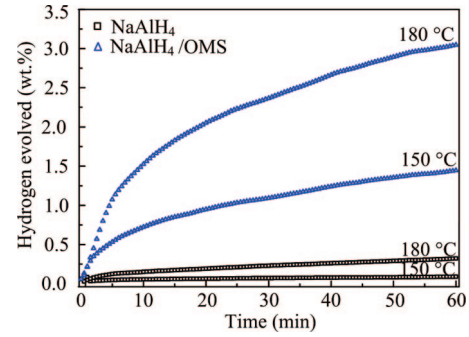

Figure 5. Dehydrogenation curves for the pristine $NaAlH_4$ and the $NaAlH_4$/OMS at 150 and 180 °C.

limited to being nanoscale by the pores of the OMS, which in turn explains why no diffraction peaks from the NaH and Al phases were observed in the XRD patterns as described above.

Hydrogen Release Performance. The DSC traces for pristine $NaAlH_4$ and $NaAlH_4$/OMS are compared in Figure 4. For pristine $NaAlH_4$, the first endothermic process at about 183 °C mainly results in the melting of $NaAlH_4$, despite some slight release of hydrogen (see TG curve below). The second one occurs over a wide temperature range with a weak peak at around 240 °C (marked by arrow), which arises from the dehydrogenation of $NaAlH_4$ to Na_3AlH_6. The third one starts from 260 °C with a peak at 275 °C, and corresponds to the decomposition of Na_3AlH_6 into the NaH and Al phases.[29,30] For the $NaAlH_4$/OMS sample, it exhibits similar trace, but the corresponding three peaks shifted toward the lower temperatures of about 175, 225, and 265 °C, respectively. This indicates that $NaAlH_4$ is relatively destabilized when its size is reduced to the nanoscale level by the pores of OMS. Shown below in Figure 4 are the TG profiles that exhibit the two-step feature for the decomposition of $NaAlH_4$. But the total amount of hydrogen evolved from the two samples is around 4.8 wt %, less than the theoretical value of 5.5 wt % given by eqs 1 and 2. This deviation may be due to the hydration during the sample preparation and/or the experimental errors of the DSC-TG equipment. An important feature that can be found from the TG profiles is that, at a given temperature, the amount of hydrogen evolved from the $NaAlH_4$/OMS sample is generally higher than that from the pristine $NaAlH_4$.

The temperature dependence of dehydrogenation curves for the pristine $NaAlH_4$ and $NaAlH_4$/OMS samples are displayed in Figure 5, showing clearly that the kinetics is greatly enhanced when $NaAlH_4$ is confined by the mesopores of OMS. The hydrogen evolved from the pristine $NaAlH_4$ is negligible at 150 °C, and less than 0.3 wt % at 180 °C in 60 min. But the corresponding values for the $NaAlH_4$/OMS sample increases to 1.4 and 3.0 wt %, respectively. To confirm this, these two samples were fully dehydrogenated and then rehydrogenated under mild conditions of 125 °C and 3.5 MPa H_2 pressure for 3 h. Afterward, they were dehydrogenated at 150 and 180 °C again, and the kinetic

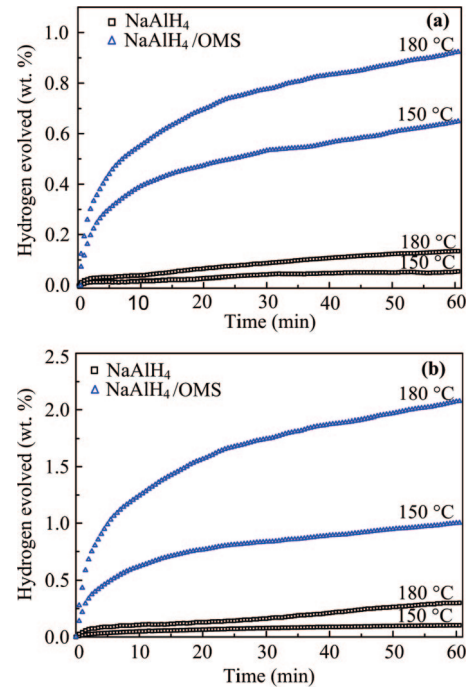

Figure 6. Dehydrogenation curves for the rehydrogenated samples: (a) hydrogenation at 125 °C and 3.5 MPa H_2 pressure for 3 h and (b) hydrogenation at 150 °C and 5.5 MPa H_2 pressure for 3 h.

curves are compared in Figure 6. Similarly, Figure 6a shows that the pristine $NaAlH_4$ sample gives off almost no hydrogen at 150 °C and less than 0.1 wt % at 180 °C in 60 min, below the corresponding values of 0.6 and 0.9 wt % for the $NaAlH_4$/OMS sample. Here, it is worth noting that in the absence of any catalyst such as Ti-containing agents,[5,12,31] the rehydrogenation in a $NaAlH_4$ system with nanoscale particles and phases is observed to occur under such milder conditions than the severe ones of 200−400 °C and 10−40 MPa reported previously.[32] With the raising of the hydrogenation temperature and pressure up to 150 °C and 5.5 MPa (see Figure 6b), the values remain unchanged for the pristine $NaAlH_4$ sample, but increase further to 1.0 wt % at 150 °C and 2.0 wt % at 180 °C, respectively, for the $NaAlH_4$/OMS sample. Therefore, it can be said that the space-confined $NaAlH_4$ in the mesopores of the OMS show better reversibility than the pristine one.

(29) Dilts, J. A.; Ashby, E. C. *Inorg. Chem.* **1972**, *11*, 1230.
(30) Claudy, P.; Bonnetot, B.; Chhine, G.; Letoffe, J. M. *Thermochim. Acta* **1980**, *38*, 75.
(31) Bogdanović, B.; Felderhoff, M.; Kaskel, S.; Pommerin, A.; Schlichte, K.; Schüth, F. *Adv. Mater.* **2003**, *15*, 1012.
(32) Dymova, T. N.; Eliseeva, N. G.; Bakum, S. I.; Degachev, Y. M. *Dokl. Akad. Nauk SSSR* **1974**, *215*, 1369.

The reasons for the results above can be understood from three aspects: (i) as the mass transfer of the solid phases is the rate-limiting step for the de-/rehydrogenation process,[33,34] the $NaAlH_4$ at a nanoscale level reduces the interdiffusion length of the constituents; (ii) the nanosized $NaAlH_4$ is thermodynamically less stable because of higher specific surface areas than the bulk one.[35] This is evidenced by a reduced temperature for dehydrogenation being found in the case of $NaAlH_4$ nanoparticles deposited on carbon nanofiber,[20] and (iii) since the starting $NaAlH_4$ particles are physically confined inside the mesopores of OMS, the resulting Na_3AlH_6, Al, and NaH phases are prevented from segregation to the large particles during the following dehydrogenation, as proven by XRD and HRTEM in the above. Such features in microstructure are in turn to facilitate the rehydrogenation. In support of this, the lessening of the phase segregation by the presence of carbon has been reported to be responsible for the enhanced performance in hydrogen storage in carbon-doped $NaAlH_4$.[36,37]

Conclusions

In summary, the present work demonstrates clearly that the space-confined $NaAlH_4$ in the pores of OMS shows the lower temperature and faster kinetics for dehydrogenation than that of the pristine one. Moreover, in the absence of a catalyst, the rehydrogenation in a dehydrogenated $NaAlH_4$ system with nanoscale particles and phases can be achieved even under milder conditions. These are because the $NaAlH_4$ particles and the resulting Al and NaH phases are controlled to be nanoscale by the pores of OMS. This method of space-confining nanoparticles may provide an approach to improve the hydrogen storage properties, in particular, the cycling stability of $NaAlH_4$ and other complex hydrides.

Acknowledgment. This work was supported by the National Science Foundation of China (No. 50571026, No. 10776004) and the Ministry of Science and Technology of China (No. 2006AA05Z126, No. 2007CB209700).

CM8002063

(33) Schüth, F.; Bogdanović, B.; Felderhoff, M. *Chem. Commun.* **2004**, *20*, 2249.
(34) Bellosta von Colbe, J. M.; Schmidt, W.; Felderhoff, M.; Bogdanović, B.; Schüth, F. *Angew. Chem., Int. Ed.* **2006**, *45*, 3663.
(35) Fichtner, M. *Adv. Eng. Mater.* **2005**, *7*, 443.
(36) Dehouche, Z.; Lafi, L.; Grimard, N.; Goyette, J.; Chahine, R. *Nanotechnology* **2005**, *16*, 402.
(37) Cento, C.; Gislon, P.; Bilgili, M.; Masci, A.; Zheng, Q.; Prosini, P. P. *J. Alloys Compd.* **2007**, *437*, 360.